Gas Sorption in New Fluorine Containing Polynorbornenes with Imide Side Chain Groups

Mikhail Tlenkopatchev, Joel Vargas, and Marco A. Almaraz-Girón

Instituto de Investigaciones en Materiales, Universidad Autónoma de México, Apartado Postal 70-360 CU, Coyoacán, México DF 04510, México

Mar López-González and Evaristo Riande*

Instituto de Ciencia y Tecnología de Polímeros (CSIC), 28006 Madrid, Spain

Received September 17, 2004

ABSTRACT: The synthesis of (*N*-3,5-bis(trifluoromethyl)phenyl-*exo*-*endo*-norbornene-5,6-dicarboximide) as well as the ring opening methatesis polymerization (ROMP) of this monomer to yield poly(*N*-3,5-bis-(trifluoromethyl)phenyl-*exo*-*endo*-norbornene-5,6-dicarboximide) are reported. The glass transition of the polymer is 162 °C. Solubility coefficients of different gases (nitrogen, oxygen, carbon monoxide, carbon dioxide, methane, ethane, ethylene, propane, and propylene) in membranes prepared by casting from poly(*N*-3,5-bis(trifluoromethyl)phenyl-*exo*-*endo*-norbornene-5,6-dicarboximide) solutions were measured at several temperatures and pressures. The interpretation of the sorption results by the dual-mode model gives the Henry and Langmuir contributions to the solubility. As usual in glassy membranes, sorption processes are exothermic and the activation energies associated with the Henry and Langmuir parameters are also negative. Gas sorption in the continuous amorphous phase was interpreted in terms of the Flory−Huggins theory obtaining reasonable values for the enthalpic parameter χ that accounts for the gas (in liquid form)−polymer interactions. The use of this approach to simulate gas sorption in polymers is discussed.

Introduction

Monte Carlo methods have been described to simulate the solubility coefficient of gases in glassy membranes.[1,2] The method assumes the statistical weight associated with the insertion of a molecule of gas in a membrane as being the product of two statistical weights related, respectively, with the variation of chemical potential of the gas inside the membrane, under a pressure p, and with the variation of the free energy of the polymer by effect of the molecule of gas insertion. In the same way, the statistical weights associated with desorption or elimination of a molecule of gas in the membrane can be determined. A shortcoming of the method is not to consider local molecular motions of the chains. Despite this, the simulation predicts the concavity with respect to the abscissa axis of the curves representing the variation of the concentration of gas in the membrane with pressure.[1,2]

An alternative method to interpret gas solubility in glassy membranes is to assume the component of the solubility coefficient governed by Henry's law as described by the Flory−Huggins theory of polymer−liquid solutions.[3,4] Using this approach, the variation of free energy arising from the mixture of gas in liquid form and polymer allows obtaining an expression that further leads to an equation relating the Henry solubility with the polymer−gas thermodynamic interaction parameter, χ. By comparing the theoretical and experimental values of Henry's constant, the value of χ can in principle be obtained.[5,6]

There has been considerable interest in recent times in the study of the performance of polynorbornenes for gases separation.[7−12] This interest arises from the easiness with which the chemical structure of this sort of polymers can be modified thus facilitating the study of the influence of chemical structure on gas transport in membranes.[13−15] Moreover gas transport and selectivity is enhanced by high order tacticity in unsubstituted polynorbornenes.[16] However, substituted polynorbornenes exhibit lower permselectivity than polyimides, one of the materials that exhibit better gas separation performance.[17,18] We have already reported gas transport results in polynorbornenes containing imide groups in their structure.[5,19] Permeation data in membranes prepared from these polymers show an enhancement of the selectivity, though the permeability remains low. The information at hand suggests that the presence of fluorine atoms in the structure of membranes of polynorbornenes enhances gas permeability across them.[10] Therefore, we have proceeded to the synthesis of poly(*N*-3,5-bis(trifluoromethyl)phenyl-*exo*-*endo*-norbornene-5,6-dicarboximide) (PNFBN), a new polymer. As a first step for the study of the performance of PNFBN for gas separation we have undertaken a thorough investigation on gas solubility in this polymer. We have measured the solubility coefficients of N_2, O_2, CO, CO_2, CH_4, C_2H_4, C_2H_6, C_3H_6, and C_3H_8 in membranes as a function of pressure and temperature, and the pertinent results were interpreted using the dual mode model thus determining the effect of temperature on Henry's constant, the Langmuir gas capacity and the affinity parameter. The Henry constant was further estimated using the Flory−Huggins theory of polymer−liquid solutions to obtain information on the enthalpic polymer gas interaction occurring in the continuous phase of the membrane assumed by the dual-mode model. The results obtained in this study open new routes to the simulation of gases solubility in glassy membranes as a function of chemical structure, which will be discussed in this work.

10.1021/ma0480751 CCC: $30.25
Published on Web 02/23/2005

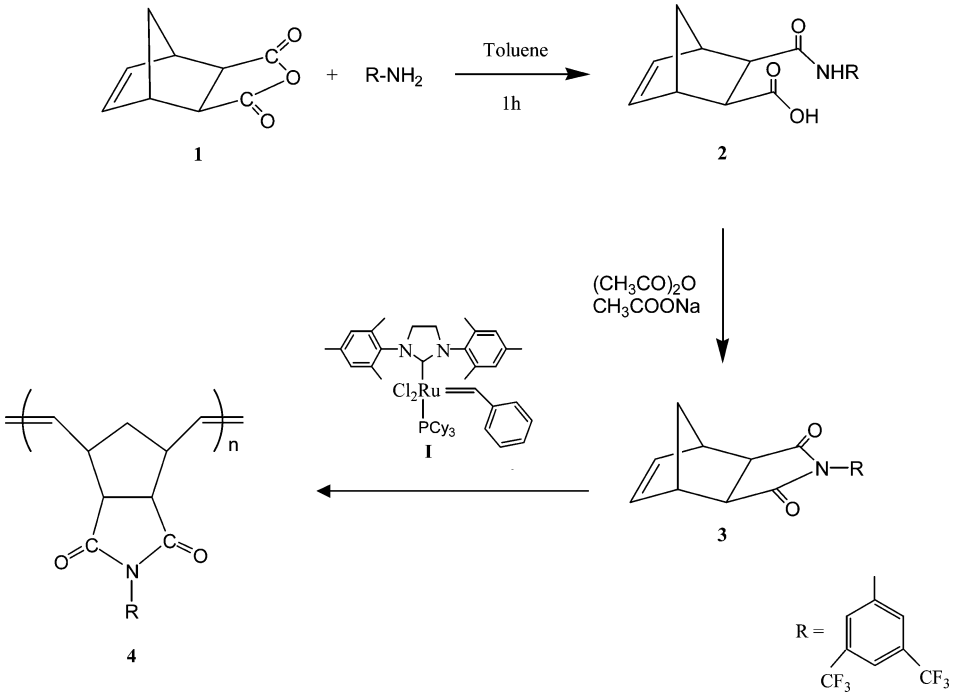

Figure 1. Scheme of the synthesis route of *exo-endo-N*-3,5-bis(trifluoromethyl)phenylnorbornene-5,6-dicarboximide and further polymerization of the monomer.

Experimental Section

Materials. A mixture of *exo-* (60%) and *endo-* (40%) norbornene-5,6-dicarboxylic anhydride (NDA, **1**) was prepared via Diels−Alder condensation of cyclopentadiene and maleic anhydride.[20] 3,5-Bis(trifluoromethyl)aniline and other chemicals were purchased from Aldrich Chemical Co. 1,2-Dichloroethane and toluene were dried over anhydrous calcium chloride and distilled under nitrogen over CaH_2. Catalyst **I**, 1,3-bis(2,4,6-trimethylphenyl)-4,5-dihydroimidazol-2-ylidene) (PCy_3)CI_2Ru=CHPh was purchased from Strem Chemical Co. and used as received.

Characterization. ^{1}H NMR and ^{13}C NMR spectra were recorded with a Varian spectrometer at 300 and 75.5 MHz, respectively, in $CDCl_3$ using tetramethylsilane (TMS) as internal standard.

The glass transition temperature was measured with a Du Pont 2100 instrument, at a heating rate of 10 °C/min. The samples were encapsulated in standard aluminum DSC pans in duplicate. Each pan was run twice on the temperature range 30−300 °C. FTIR spectra were obtained on a Nicolet 510 p spectrometer. Molecular weights and molecular weight distributions with reference to polystyrene standards were determined on a Varian 9012 GPC instrument at 30 °C in chloroform (universal column and a flow rate of 1 mL min^{-1}).

Monomer Synthesis. *N*-3,5-Bis(trifluoromethyl)phenyl-*exo-endo*-norbornene-5,6-dicarboximide (FPhNDI, **3**). NDA, **1** (12 g, 70 mmol), was dissolved in 120 mL of toluene. An amount of 11 g (72 mmol) of 3,5-bis(trifluoromethyl)aniline in 120 mL of toluene is added dropwise to the stirred solution of *exo*-NDA. The reaction was maintained at 70 °C for 1 h and then cooled to room temperature. A precipitate was filtered, and dried to give 22 g (70 mmol) of amic acid. The obtained amic acid **2** (22 g, 70 mmol), anhydrous sodium acetate (3.3 g, 40 mmol), and acetic anhydride (65 g, 640 mmol) were heated at reflux for 2 h and then cooled. The solid, which is crystallized out on cooling, was filtered, washed several times with water, and dried in a vacuum oven at 50 °C overnight. Pure monomer **3** (Figure 1) was obtained after two recrystallizations from hexane: yield = 87%, mp = 216−218 °C. ^{1}H NMR (300 MHz, $CDCl_3$) (Figure 2): δ (ppm) = 7.86−7.69 (3H, m), 6.21-(2H, t), 6.31(2H, t), 3.55−3.47 (2H, m), 2.82 (2H, t), 1.85−1.60 (2H, m). ^{13}C NMR (75 MHz, $CDCl_3$): δ (ppm) = 175.80, 134.76, 126.67, 124.54, 122.09, 52.41, 45.92, 45.65. FT-IR: 3064 (C=C−H str), 2946 (C−H asym str), 2877 (C−H sym str), 1710 (C=O), 1594 (C=C str), 1454 (C−H def.), 1382 (=CH− def.), 1329 (C−H def.), 1289 (C−H def.), 1188 (C−N str), 975 (C−C skel.), 799 cm^{-1} (C=C−H def.).

Monomer Metathesis Polymerization. Ring opening methatesis polymerizations were carried out in glass vials under a dry nitrogen atmosphere at room temperature. Adding ethyl vinyl ether under a nitrogen atmosphere terminated the reactions. After cooling, the solutions were poured into an excess of methanol. The polymer was purified by solubilizing into chloroform containing few drops of 1 N HCl and precipitating into methanol. The polymer was dried in a vacuum oven at 40 °C to constant weight.

Polymer Synthesis. Poly(*N*-3,5-bis(trifluoromethyl)phenyl-*exo-endo*-norbornene-5,6-dicarboximide) (Poly(FPhNDI), **4**). 1 g (3.36 mmol) of **3** and 0.0033 g (0.0033 mmol) of catalyst **I** were stirred in 3.4 mL of 1,2-dichloroethane at room temperature for 2 h. The polymer obtained was soluble in chloroform, toluene, and dichloromethane. ^{1}H NMR (300 MHz, $CDCl_3$): δ (ppm) = 7.86−7.69 (3H, m), 6.04 (2H, s, trans), 5.78 (2H, s, cis), 3.48 (2H, s), 2.86 (2H, m), 1.68 (2H, m). ^{13}C NMR (75 MHz, $CDCl_3$): δ (ppm) = 177.19, 132.93, 129.11, 128.32, 126.36, 50.38, 46.20, 42.32. FT-IR: 3034, 2938, 2879, 1775, 1598, 1459, 1365, 1329, 1295, 1165, 980, 790 cm^{-1}.

The values of the number-average molecular weight, M_n, heterodispersity index, M_w/M_n, and glass transition temperature of poly(*exo-endo-N*-3,5-bis(trifluoromethyl)phenylnorbornene-5,6-dicarboximide) were, respectively, 2.2×10^5, 1.2, and 162 °C.

Sorption Measurements. Films of poly(*exo-endo-N*-3,5-bis(trifluoromethyl)phenylnorbornene-5,6-dicarboximide) obtained by casting from polymer solutions in chloroform were used in the sorption measurements. The evaporation of the solvent proceeded overnight and then the rest of solvent in the film was eliminated in high vacuum at 30 °C.

The concentration of gas in the films was measured at constant temperature with an experimental device formed by a gas reservoir separated from the sorption chamber by a valve.[21] The reservoir and the sorption chamber equipped, respectively, with Gometrics (0−35 bar) and Ruska model 7230 [(0−35) $\times$ 10^3 Torr] pressure sensors were immersed in a thermostat at the temperature of interest. At the beginning, polymer films were placed inside the sorption chamber and

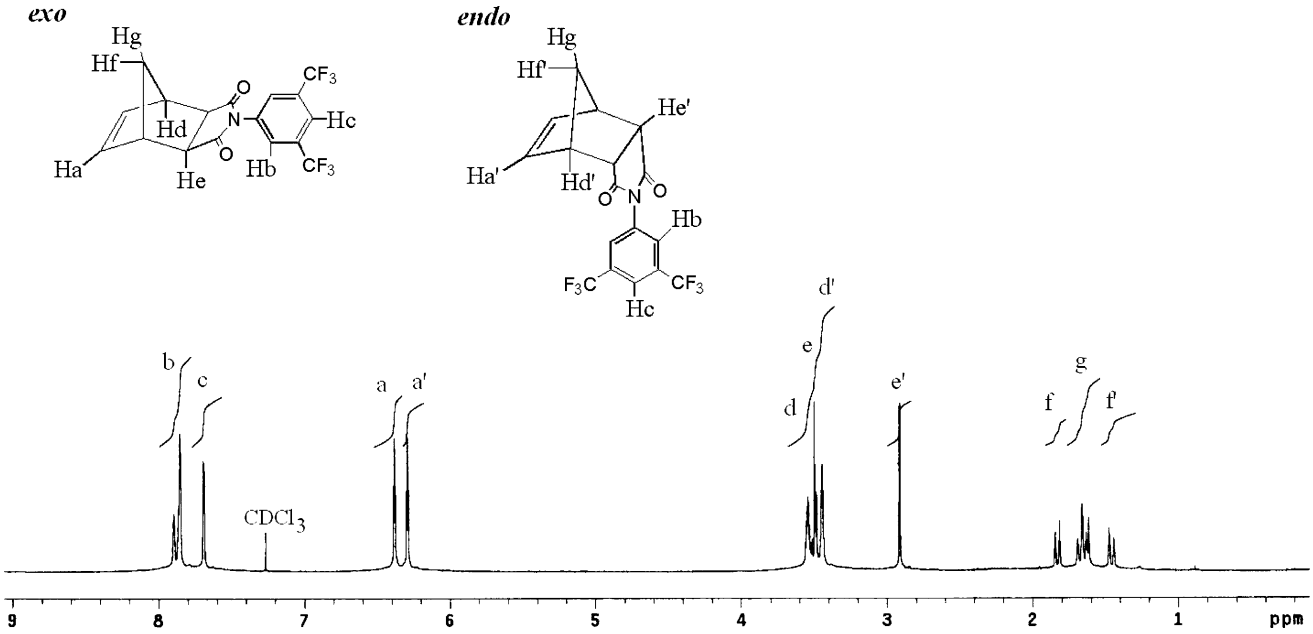

Figure 2. ^{1}H NMR spectrum of *exo-endo-N*-3,5-bis(trifluoromethyl)phenylnorbornene-5,6-dicarboximide.

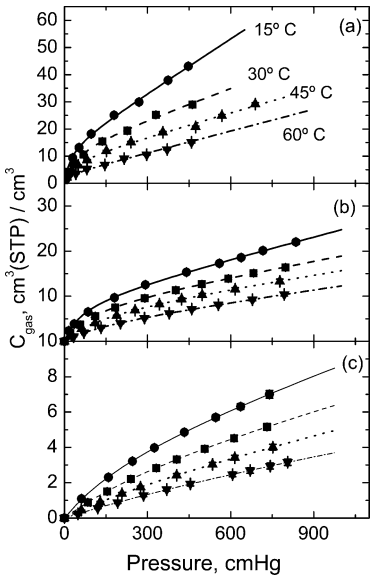

Figure 3. Variation of the concentrations of (a) propylene, (b) ethylene, and (c) methane in poly(*exo-endo-N*-3,5-bis-(trifluoromethyl)phenylnorbornene-5,6-dicarboximide) with pressure, at the temperatures indicated in part a.

exposed to vacuum about 6 h, at 60 °C, to remove air or any other gas proceeding from a preceding experiment. Then the pertinent gas, at a given pressure, was introduced into the reservoir, and once it reached the temperature of interest, the valve separating the reservoir and the sorption chamber was suddenly opened and closed. The decrease of the pressure of the gas in the sorption chamber was recorded every second with a PC via a precision pressure indicator. Once the pressure was constant, an additional amount of gas was introduced into the sorption chamber and then allowed to come again to equilibrium, and so on. In this way, gas sorption was measured as a function of pressure using compressibility factors to determine the concentration of gas in the films. The sorption measurements were performed at several pressures in the temperature range 15−60 °C, with the exception of oxygen, for which the interval of temperature was 2−45 °C. Pressure leaks and the adsorption of gas in the chamber walls were previously measured in blank experiments.

General Sorption Results. Illustrative isotherms showing the pressure dependence of the concentration of propylene, ethylene and methane in PNFBN films are shown at several temperatures in Figure 3. The curves exhibit the usual pattern displayed by the sorption of gases in glassy polymers, that is, the isotherms are concave with respect to the abscissa axis. Similar patterns exhibit the isotherms representing the pressure dependence of the concentration of carbon dioxide, ethane and propane. For comparative purposes isotherms showing the concentration of these latter gases, at 30 °C, are shown as a function of pressure in Figure 4. The contribution of Langmuir sites to the sorption process is nearly negligible for the less condensable gases (O_2, N_2, and CO). Illustrative plots for the sorption of oxygen in PNFBN films are shown in Figure 5. It is worth noting that the isotherm at 2 °C of oxygen exhibits a weak concavity that disappears at higher temperatures.

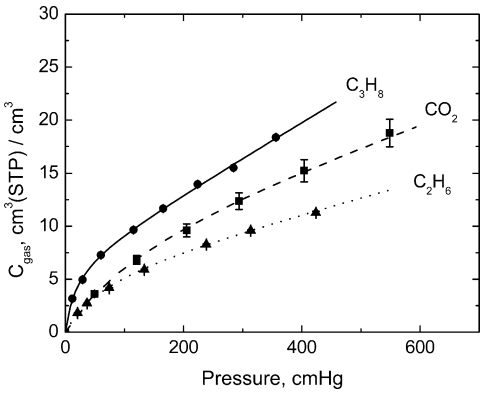

Figure 4. Variation of the concentrations of (a) propane, (b) carbon dioxide, and (c) ethane in poly(*exo-endo-N*-3,5-bis-(trifluoromethyl)phenylnorbornene-5,6-dicarboximide) with pressure, at 30 °C.

The solubility coefficient of the most condensable gases (CO_2, CH_4, C_2H_6, C_2H_4, C_3H_6, and C_3H_8) is characterized for undergoing a sharp decrease with increasing pressure in the region of low pressures. At moderate pressures the solubility coefficient only slightly decreases as the pressure goes up, eventually reaching a constant value in the high-pressure limit. This behavior is described by the dual-mode model, which expreses the pressure dependence of the solubility coefficient in glassy polymers by[22]

$$S = k_D + \frac{bC'_H}{1 + bp} \quad (1)$$

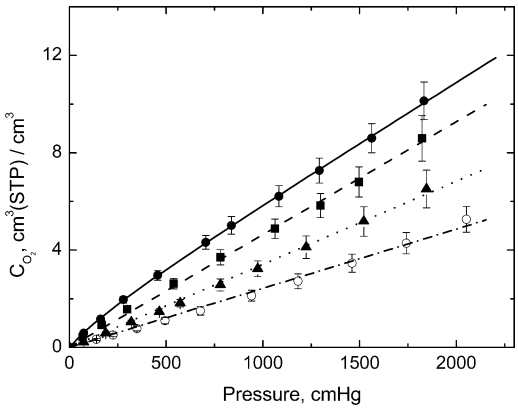

Figure 5. Sorption behavior of oxygen in poly(*exo-endo-N*-3,5-bis(trifluoromethyl)phenylnorbornene-5,6-dicarboximide), at (●) 2, (■) 15, (▲) 30, and (○) 45 °C.

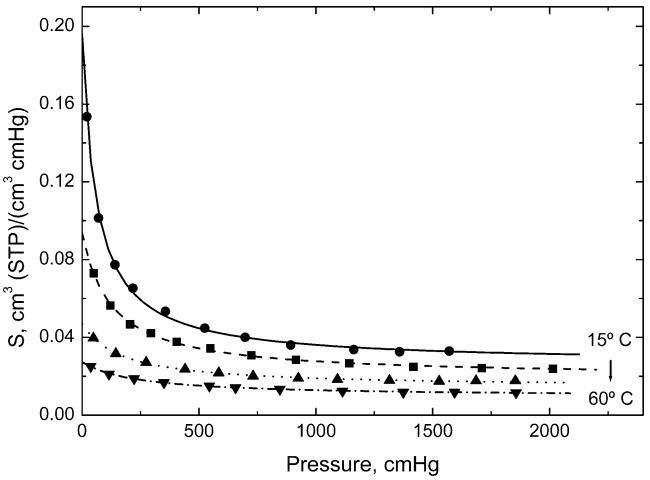

Figure 6. Variation of the sorption coefficient of carbon dioxide in poly(*exo-endo-N*-3,5-bis(trifluoromethyl)phenylnorbornene-5,6-dicarboximide) at several temperatures.

where k_D is the solubility coefficient of the gas in the continuous phase of the glassy material, C'_H is the concentration of gas immobilized in Langmuir sites, and b is an affinity parameter accounting for the sorption/desorption ratio. The drop in the values of the solubility coefficient in the low-pressure region is higher the lower is the temperature (see Figure 6). As pressure increases, the drop in the values of S decreases as temperature goes up. The variation of the values of the solubility coefficient at 1 bar and 30° C follows the trends $S(C_3H_6) > S(C_3H_8) > S(CO_2) > S(C_2H_6) > S(C_2H_4) > S(CH_4) > S(CO) > S(O_2) > S(N_2)$. The values of the dual mode model parameters that fit eq 1 to the experimental isotherms representing the variation of the concentration of gas with pressure are given in Table 1. It can be seen that in general k_D, b, and C'_H decrease with increasing temperature. The values of Henry's constant are strongly dependent on gas condensability following the same trends as the solubility coefficient, that is, $k_D(C_3H_6) > k_D(C_3H_8) > k_D(CO_2) > k_D(C_2H_6) > k_D(C_2H_4) > k_D(CO) \cong k_D(CH_4) > k_D(O_2) > k_D(N_2)$. It is worth noting that the parameter b that accounts for the gas polymer affinity is rather high for the most condensable polymers if as comparison basis the value of b for gases of low condensability, such as methane, is taken. Arrhenius plots for the solubility coefficients of different gases at 1 bar, shown in Figure 7, are straight lines and the corresponding sorption enthalpies obtained from the slopes of the plots are given in Table 2. As usual, the results indicate that gas sorption in glassy polymers

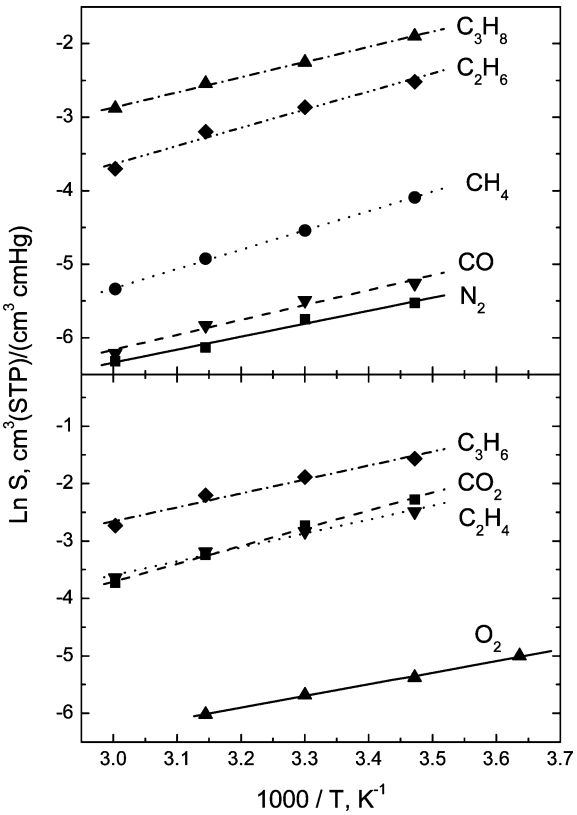

Figure 7. Arrhenius plots for the solubility coefficients of the gases indicated in poly(*exo-endo-N*-3,5-bis(trifluoromethyl)-phenylnorbornene-5,6-dicarboximide).

Table 1. Values of the Dual Mode Parameters, at Different Temperatures, for the Sorption of Different Gases in PNFBN Membranes

gas	parameters	15 °C	30 °C	45 °C	60 °C
propane	$10^3 \times k_D$, cm^3(STP)/(cm^3 cmHg)	49.8 ± 3.0	33.1 ± 1.3	27.1 ± 1.3	16.2 ± 1.7
	C'_H, cm^3(STP)/cm^3	9.2 ± 0.5	6.8 ± 0.4	5.4 ± 0.4	6.1 ± 0.9
	$10^3 \times b$, (cmHg)$^{-1}$	60.6 ± 6.1	53.3 ± 8.9	35.5 ± 8.0	13.2 ± 3.1
propylene	$10^3 \times k_D$, cm^3(STP)/(cm^3 cmHg)	65.9 ± 3.2	37.1 ± 3.8	29.1 ± 1.8	23.7 ± 1.2
	C'_H, cm^3(STP)/cm^3	14.1 ± 1.4	13.4 ± 1.8	8.9 ± 1.1	4.2 ± 0.5
	$10^3 \times b$, (cmHg)$^{-1}$	44.1 ± 11.8	24.4 ± 6.9	29.1±9.2	39.3 ± 13.8
ethane	$10^3 \times k_D$, cm^3(STP)/(cm^3 cmHg)	15.3 ± 0.8	14.6 ± 0.9	9.4 ± 0.6	9.9 ± 2.7
	C'_H, cm^3(STP)/cm^3	7.6 ± 0.4	6.1 ± 0.5	5.6 ± 0.4	3.4 ± 2.1
	$10^3 \times b$, (cmHg)$^{-1}$	25.2 ± 3.1	15.0 ± 2.0	9.7 ± 1.0	6.6 ± 5.1
ethylene	$10^3 \times k_D$, cm^3(STP)/(cm^3 cmHg)	15.9 ± 0.5	11.1 ± 0.3	9.5 ± 0.4	8.7 ± 0.3
	C'_H, cm^3(STP)/cm^3	9.5 ± 0.4	8.6 ± 0.3	7.1 ± 0.4	4.2 ± 0.3
	$10^3 \times b$, (cmHg)$^{-1}$	15.3 ± 1.4	9.6 ± 0.6	6.8 ± 0.6	6.2 ± 0.7
methane	$10^3 \times k_D$, cm^3(STP)/(cm^3 cmHg)	5.3 ± 0.3	4.0 ± 0.2	3.6 ± 0.1	2.5 ± 0.5
	C'_H, cm^3(STP)/cm^3	4.3 ± 0.4	3.6 ± 0.3	2.2 ± 0.3	2.7 ± 1.4
	$10^3 \times b$, (cmHg)$^{-1}$	3.3 ± 0.4	2.1 ± 0.2	1.9 ± 0.2	0.9 ± 0.4
carbon dioxide	$10^3 \times k_D$, cm^3(STP)/(cm^3 cmHg)	25.3 ± 0.8	18.8 ± 0.4	15.2 ± 0.4	9.8 ± 0.3
	C'_H, cm^3(STP)/cm^3	11.1 ± 1.1	10.2 ± 0.8	4.1 ± 0.6	3.6 ± 0.5
	$10^3 \times b$, (cmHg)$^{-1}$	14.6 ± 4.4	6.9 ± 1.3	10.6 ± 4.7	5.7 ± 1.8

Table 2. Activation Energies Associated with Henry's Constant, k_D, and Solubility Coefficient, S, for Different Gases

gas	ΔE_k, kcal/mol	ΔH_s, kcal/mol
O_2	-4.1 ± 0.1	-4.1 ± 0.1
N_2	-3.5 ± 0.3	-3.5 ± 0.3
CO_2	-3.9 ± 0.5	-6.2 ± 0.3
CO	-4.1 ± 0.4	-4.1 ± 0.4
CH_4	-3.1 ± 0.5	-5.4 ± 0.1
C_2H_6	-2.3 ± 0.8	-4.9 ± 0.5
C_2H_4	-2.6 ± 0.5	-4.8 ± 0.4
C_3H_8	-4.5 ± 0.6	-4.1 ± 0.1
C_3H_6	-4.3 ± 0.7	-4.9 ± 0.6

is an exothermic process even for gases of low condensability.[23] The values of the sorption heats are rather close for different gases suggesting that the prefactor of the Arrhenius plots is mainly responsable for the differences observed between the solubility coefficients of the most (propane, propene, ethane, ethene, carbon dioxide) and less (nitrogen, carbon monoxide, oxygen, methane) condensable gases. The dual mode parameters also obey Arrhenius behavior with negative activation energies. Illustrative Arrhenius plots for k_D, b, and C'_H are shown in Figure 8.

Discussion

The dual mode model assumes the glassy state as formed by a continuous phase in which microvoids accounting for the excess volume are dispersed. In the continuous phase Henry's type sorption occurs while the microvoids act as Langmuir sites where gas adsorption takes place. In view of these assumptions, we could assume gas solubility in the continuous phase governed by the entropy of the gas (in the liquid state)-polymer mixture and the enthalpic contribution arising from polymer−gas interactions. The variation of chemical potential arising from the mixture of a gas A in liquid form with a polymer P can be written as[4,6]

$$\frac{\mu_{A,T} - \mu_{0A,T}}{RT} = \ln\frac{p_{A,T}}{p_{0A,T}} = \ln v_A + v_P\left(1 - \frac{\bar{V}_A}{\bar{V}_P}\right) + \chi_A v_P^2 \quad (2)$$

where $p_{0A,T}$ and $p_{A,T}$ are, respectively, the vapor pressure of the gas in the liquid state and in solution at temperature T, v_A and v_P are, respectively, the molar volume fractions of gas in the liquid state and polymer,

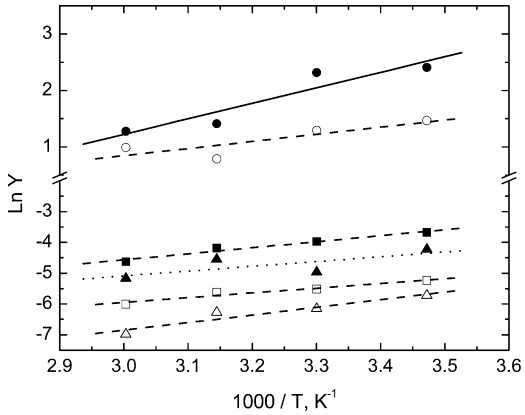

Figure 8. Typical Arrhenius plots for the dual mode parameters of carbon dioxide and methane in poly(*exo-endo-N*-3,5-bis(trifluoromethyl)phenylnorbornene-5,6-dicarboximide): (circles) C'_H or Langmuir capacity, (squares) k_D or Henry's constant, and (triangles) b or affinity parameter. Filled and open symbols refer, respectively, to carbon dioxide and methane.

Table 3. Values of the Boiling Temperatures, $T_{b,A}$, Latent Heat of Vaporization, λ, and Enthalpic Interaction Parameter, χ, for Different Gases

gas	$T_{b,A}$, K[a]	$\bar{V}_P$, cm³/mol[b]	λ, kcal/mol[a]	χ at 30 °C
N_2	72.4	35	1.330	0.45
O_2	90.2	28	1.631	0.64
CO	81.7	35.4	1.444	0.11
CO_2	194.7	46	4.112	1.04
CH_4	111.7	38	1.944	0.02
C_2H_6	185.0	55	3.50	0.52
C_2H_4	169.5	49.3	3.23	1.02
C_3H_8	231.1	76	4.477	1.10
C_3H_6	225.5	69.09	3.32	1.85

[a] Reference 24. [b] Reference 25.

respectively, and $\bar{V}_A$ and $\bar{V}_P$ are the respective molar partial volumes. The vapor pressure of a gas in the liquid form at temperature T can be estimated from the boiling temperature of the gas under 1 atm of pressure, $T_{b,A}$, yielding

$$\ln p_{0A,T} = \frac{\lambda_A}{RT_{b,A}}\left(1 - \frac{T_{b,A}}{T}\right) \quad (3)$$

where use of the Clausius−Clapeyron equation was made. In eq 3, λ_A is the latent heat of vaporization. Equations 2 and 3 lead to

$$\ln p_{A,T} = \ln(\bar{V}_A c_A) + (1 + \chi_A) - (1 + 2\chi_A)\bar{V}_A c_A + \frac{\lambda_A}{RT_{b,A}}\left(1 - \frac{T_{b,A}}{T}\right) \quad (4)$$

where $c_A = v_A/\bar{V}_A$. Since $\bar{V}_A \ll \bar{V}_P$ and $v_A \ll 1$, the terms containing $\bar{V}_A/\bar{V}_P$ and v_A^2 were neglected in the development of eq 4. The concentration of gas in the liquid form in the membrane can be obtained from eq 4 and taking into account that $S = c_A/p_{A,T}$, the solubility coefficient can be written as

$$S = k_D \exp[(1 + 2\chi_A)c_A\bar{V}_A] \quad (5)$$

where k_D in cm³(STP)/(cm³ cmHg) is given by

$$k_D = \frac{22414}{76\bar{V}_A}\exp\left[-(1 + \chi_A) - \frac{\lambda_A}{RT_{b,A}}\left(1 - \frac{T_{b,A}}{T}\right)\right] \quad (6)$$

The enthalpic parameter can in principle be obtained by means of eq 6 using the values of the latent heat of vaporization, boiling temperature, and partial molar volume given in Table 3. The pertinent results obtained for χ_A at 30 °C are also collected in Table 3. It can be seen that the enthalpic parameter is positive, its value lying in the range 0 to 1.86, depending on the type of gas. The values predicted by eq 6 for k_D come very close to the experimental ones using reasonable values for the enthalpic parameter, thus apparently validating the assumptions upon which the development of eq 6 are based. It is worth noting that the exponential term in eq 5 may become significant at big pressures, thus decreasing the immobilizing effect of the Langmuir sites on the gas molecules.

Values of the interaction parameter are plotted against the gases boiling temperature in Figure 9. It can be seen that χ_A shows a tendency to increase with increasing values of $T_{b,A}$. The logarithm of the experimental values of Henry's constant, plotted as a function of the boiling temperatures of the gases in Figure 10, is a linear function of $T_{b,A}$ as, in principle, an analysis of

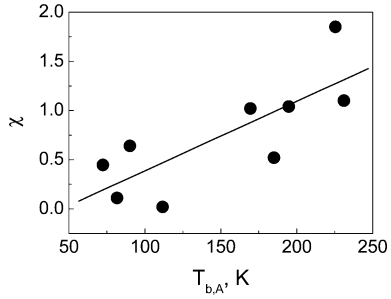

Figure 9. Variation of the enthalpic interaction gas−polymer parameter with the gases boiling temperature.

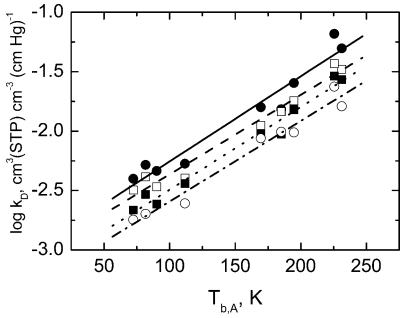

Figure 10. Plots of the Henry's sorption constant in poly(*exo-endo-N*-3,5-bis(trifluoromethyl)phenylnorbornene-5,6-dicarboximide) for propane, propylene, ethane, ethylene, methane, carbon dioxide, carbon oxide, oxygen, and nitrogen against the respective boiling temperatures, at several temperatures: (●) 15, (□) 30, (■) 45, and (○) 60 °C.

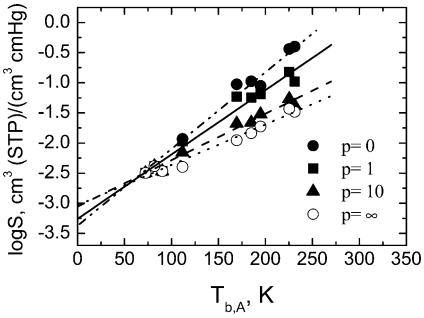

Figure 11. Arrhenius plots for the solubility coefficients of propane, propylene, ethane, ethylene, methane, carbon dioxide, carbon oxide, oxygen, and nitrogen in poly(*exo-endo-N*-3,5-bis-(trifluoromethyl)phenylnorbornene-5,6-dicarboximide) at several pressures, in cmHg: (●) 0,(■) 76, (▲) 760, and (○) ∞.

eq 6 would suggest. Actually, the average of the values of $\lambda_A/RT_{b,A}$ factor is 9.21 ± 0.82 and taking into account the rather small variations of the values of both the enthalpic parameter and the molar partial volume for different gases, eq 6 could be written at 30 °C as log k_D = constant + $3.95T_{b,A}/T$. The slope predicted by eq 6 at 30° is 1.3×10^{-2} close to that experimentally found, ca. 0.7×10^{-2}. It is worth noting that the log k_D vs $T_{b,A}$ plots at different temperatures are nearly parallel straight lines with slightly decreasing slopes with increasing temperatures as a consequence of the fact that their slopes are $3.95/T$. Values of the logarithm of the solubility coefficient at 30° are plotted as a function of $T_{b,A}$ for different pressures in Figure 11. The data also fit fairly well to straight lines whose slopes decrease as the pressure increases intersecting the ordinates axis at −3.2 ± 0.2. These results confirm the rather low contribution to solubility of Langmuir sites for the less condensable gases.

The information at hand[26,27] indicates that the lower is the working temperature the larger is C'_H. This suggests that the gas concentration in Langmuir sites at $T < T_g$ is associated with the excess volume fraction. This latter quantity can approximately be written as

$$\Delta V_{excess} = [(\alpha)_l - (\alpha)_g](T_g - T) \quad (7)$$

where $\alpha = (1/V)dV/dT$ is the expansion coefficient and the subscripts l and g refer to the rubbery and glassy states, respectively. If we assume C'_H proportional to ΔV_{excess}, the final expression for the gas concentration in Langmuir sites is given by

$$C'_H = 22414k'_H \frac{\Delta V_{excess}}{\bar{V}} = \frac{22414k'_H}{\bar{V}}(\alpha_l - \alpha_g)(T_g - T) \quad (8)$$

where $\bar{V}$ is the molar partial volume of the gas in the liquid state at temperature T and k'_H is a proportionality constant dependent on both the gas and the chemical nature of the polymer. It has been observed that eq 8 holds for the sorption process of CO_2 in homologous series of polynorbornenes.[28] Koros and co-workers[26,27] also have reported that eq 8 gives a good account of the temperature dependence of C'_H for CO_2 in glassy membranes with different chemical structure. These findings suggest that provided that $T_g - T$ is similar, the condensability of the gas rather than the chemical structure of the membrane governs the gas concentration in Langmuir sites.

The good concordance of the experimental values of k_D with those determined from eq 6 opens a new route to the simulation of gas sorption in polymers that is briefly described below. The route, based on the Widom method,[29,30] assumes the sorption chemical potential separated in an ideal gas contribution and an excess part arising from the change in free energy caused by the insertion of a gas molecule in the polymer matrix. Let us assume that the number of particles inside a cubic box of the membrane is n and the number of particles at equilibrium is N. The statistical weight associated with an additional molecule of gas in the cubic box representative of the membrane is given by

$$\sigma_{n\to n+1;i} = \exp\left[-\frac{\mu(n+1) - \mu(N)}{kT}\right]\exp\left(-\frac{\Delta F}{kT}\right) \quad (9)$$

where μ is the chemical potential of the ideal gas and ΔF represents the excess part corresponding to the change in free energy indicated above. Since

$$\mu(n) = \mu_0 + kT\ln(n/V) \quad (10)$$

where n/V is the concentration of gas in solution in equilibrium with the pressure of external gas, eq 9 becomes

$$\sigma_{n\to n+1;in} = \frac{N}{n+1}\exp\left(-\frac{\Delta F}{kT}\right) \quad (11)$$

Usually, the value of N is calculated by assuming that the box is empty so that $\sigma_{n\to n+1;in}$ can be written as[1,2]

$$\sigma_{n\to n+1;in} = \frac{pV}{(n+1)kT}\exp\left(-\frac{\Delta F}{kT}\right) \quad (12)$$

where V is the volume of the box and p is the pressure. By the same token, the statistical weight associated with the removal of a particle from a box containing n particles would be

$$\sigma_{n\rightarrow n-1;\mathrm{re}} = \frac{(n-1)kT}{pV}\exp\left(\frac{\Delta F}{kT}\right) \tag{13}$$

The values of $\sigma_{n\rightarrow n+1;\mathrm{in}}$ obtained by means of eq 11 are obviously in excess because N is calculated as whether polymer chains were not present in the cubic box. A better approach would be to estimate N from Henry's constant, which as was shown above, can be fairly well estimated from eq 6. The only unknown quantity in this equation is the enthalpic parameter for which a value of 0.5 could in principle be used. Under a pressure p, the statistical weight associated with the insertion of an additional gas molecule in the cubic box already containing n molecules, can be obtained as

$$\sigma_{n\rightarrow n+1;\mathrm{in}} = \frac{k_{\mathrm{D}}pV}{n+1}\exp\left(-\frac{\Delta F}{kT}\right) \tag{14}$$

where it was considered that

$$N \cong k_{\mathrm{D}}pV \tag{15}$$

The value of N obtained from eq 15 is in most cases the lower bound for the number of particles inside the box. Notice that according to eq 1

$$\lim_{p\rightarrow 0} S = k_{\mathrm{D}} + bC'_{\mathrm{H}}; \quad \lim_{p\rightarrow\infty} S = k_{\mathrm{D}} \tag{16}$$

For the less condensable gases (H_2, O_2, N_2, CO, etc.), $S \cong k_{\mathrm{D}}$, and therefore, the values obtained for N are in principle fairly realistic. Under a pressure p, the statistical weight associated with the removal of a molecule from the box which already contains n molecules is given by

$$\sigma_{n\rightarrow n-1;\mathrm{re}} = \frac{n-1}{k_{\mathrm{D}}pV}\exp\left(\frac{\Delta F}{kT}\right) \tag{17}$$

Further normalization of the insertion and removal statistical weights given by eqs 14 and 17 leads to the insertion and removal probabilities which, in conjunction with Monte Carlo techniques, can be used to compute gas sorption in glassy membranes as a function of chemical structure. Work is in progress to test the reliability of this approach.

The permselectivity or factor of separation for two gases depends on the sorption and diffusive processes taking place in gas transport. The contribution of the sorption process to permselectivy is given by $S_{\mathrm{A}}/S_{\mathrm{B}}$ where A and B are the gases to be separated. An inspection of the values of Table 1 shows that solubility is a poor permselectivity factor for condensable gases. For example, taking propylene as A, the values of $S_{\mathrm{A}}/S_{\mathrm{B}}$ are lower than 2 if B is propane, ethane, ethylene, and carbon dioxide. However, the performance of the selectivity factor is fairly good for the less condensable gases for which $S_{\mathrm{A}}/S_{\mathrm{B}}$ may reach values so high as 35, 33, 28, and 10 for nitrogen, oxygen, carbon monoxide, and methane, respectively. The logarithm of the diffusion coefficients of gases through glassy membranes is a decreasing linear function of the size of the diffusants while the logarithm of the sorption coefficients is an increasing linear function of gas molecules size. Therefore, to optimize the separation of condensable gases from the less condensable ones requires that $D_{\mathrm{A}}/D_{\mathrm{B}} \ll S_{\mathrm{A}}/S_{\mathrm{B}}$, where D is the diffusion coefficient. Work dealing with the diffusive characteristics of the membranes used in this study will be published later.

Conclusions

The critical interpretation of the solubility of O_2, N_2, CO, CO_2, CH_4, C_2H_4, C_2H_6, C_3H_6, and C_3H_8 in glassy membranes prepared by casting from chloroform solutions of poly(*N*-3,5-bis(trifluoromethl)phenyl-*exo-endo*-norbornene-5,6-dicarboximide) shows that gas solution in the continuous phase of the membrane assumed by the dual mode model can be determined from the gas (in the liquid state)−polymer mixing free energy usually utilized in very concentrated polymer−liquid solutions. This approach leads to an expression relating Henry's contribution to the solubility with both the enthalpic interaction parameter and the boiling point of the gases. Reasonable values of the enthalpic interaction gas (in the liquid state)−polymer parameter are obtained which exhibit a tendency to increase as the molecule gas size increases. The Flory−Huggins approach allows to predict reasonably well the dependence of the Henry's constant on the boiling temperature of the gases at 1 bar. Also, the logarithm of the solubility coefficient for different gases is a linear function of their respective boiling temperatures. Methods are outlined to improve the simulation of gas sorption in glassy membranes.

Acknowledgment. We thank the CONACyT for generous support of this research with Contract No. NC-204. Financial support provided by the DGICYT (Dirección General de Investigación Científica y Tecnológica) through Grant MAT2002-04042-C02-02 is also gratefully acknowledged.

References and Notes

(1) Tiemblo, P.; Saiz, E.; Guzmán, J.; Riande, E. *Macromolecules* **2002**, *35*, 4167.
(2) Saiz, E.; López-González, M. M.; Riande, E.; Guzmán, J.; Compañ, V. *Phys. Chem. Chem. Phys.* **2003**, *5*, 2862.
(3) Flory, P. J. *Principles of Polymer Chemistry*; Cornell University Press: Ithaca, NY, 1953; Chapter 21.
(4) Petropoulos, J. H. *Pure Appl. Chem.* **1993**, *65*, 219.
(5) Tlenkopatchev, M. A.; Vargas, J.; López González, M. M.; Riande, E. *Macromolecules* **2003**, *36*, 8483.
(6) López-González, M. M.; Compañ, V.; Riande, E. *Macromolecules* **2003**, *36*, 8576.
(7) Kawakami, Y.; Toda, H.; Higashino, M.; Yamashita, Y. *Polym. J.* **1988**, *4*, 285.
(8) Bondar, V. I.; Kukharskii, Yu. M.; Yampol'skii, Yu. P.; Finkelshtein, E. Sh.; Makovetskii, K. L. *J. Polym. Sci., Part B: Polym. Phys.* **1993**, *31*, 1273.
(9) Chun-thian, Z.; do Rosário Ribeiro, M.de Pinho, M. N.; Subrahmanyam, V. S.; Gil, C. L.; de Lima, A. P. *Polymer* **2001**, *42*, 2455.
(10) Yampol'skii, Yu. P.; Bespalova, N. B.; Finkelshtein, E. Sh.; Bondar, V. I.; Popov, A. V. *Macromolecules* **1994**, *27*, 2872.
(11) Finkelshtein, E. Sh.; Gringolts, M. L.; Ushakov, N. V.; Lakhtin, V. G.; Soloviev, S. A.; Yampol'skii, Yu. P. *Polymer* **2003**, *44*, 2843.
(12) Dorkenoo, K. D.; Pfromm, P. H.; Rezac, M. E. *J. Polym. Sci., Part B: Polym. Phys.* **1998**, *36*, 797.
(13) Tlenkopatchev, M. A.; Fomine, S.; Miranda, E.; Fomina, L.; Ogawa, T. *Polym. J.* **1995**, *27*, 1173.
(14) Thenkopatchev, M. A.; Fomine, S.; Fomina, L.; Gaviño, R.; Ogawa, T. *Polym. J.* **1997**, *29*, 622.
(15) Maya, V. G.; Contreras, A. P.; Canseco, M. A.; Tlenkopatchev, M. A. *React. Funct. Polym.* **2001**, *49*, 145.
(16) Steinhäusler, T.; Koros, W. J. *J. Polym. Sci., Part B: Polym. Phys.* **1997**, *35*, 91.

(17) Kesting, R. E.; Fritzsche, A. K. *Polymeric Gas Separation Membranes*; Wiley-Interscience: New York, 1993.
(18) Ohya, H.; Kudryavtsev, V. V.; Senova, S. I. *Polyimide Membranes*; Gordon & Breach Publishers: Tokyo, 1996.
(19) Contreras, A. P.; Tlenkopatchev, M. A.; López-González, M. M.; Riande, E. *Macromolecules* **2002**, *35*, 4677.
(20) Kastner, K. F.; Calderon, N. J. *J. Mol. Catal.* **1982**, *15*, 47.
(21) Koros, W. J.; Paul, D. R.; Rocha, A. A. *J. Polym. Sci., Polym. Phys. Ed.* **1976**, *14*, 687.
(22) Vieth, W. R.; Sladek, K. J. *J. Colloid Sci.* **1965**, *20*, 1014. Ref 17; p 60.
(23) van der Vegt, N. F. A. *J. Membr. Sci.* **2002**, *205*, 125.
(24) *International Critical Tables*; 1928; Vol. III.
(25) Merkel, T. C.; Bondar, V. I.; Nagai, K.; Freeman, B. D.; Pinnau, I. *J. Polym. Sci., Part B: Polym. Phys.* **1998**, *38*, 415.
(26) Koros, W. J.; Paul, D. R. *J. Polym. Sci., Polym. Phys. Ed.* **1978**, *16*, 1947.
(27) Muruganandam, N.; Koros, W. J.; Paul, D. R. *J. Polym. Sci., Part B: Polym. Phys.* **1987**, *25*, 1999.
(28) Yampol'skii, Yu. P.; Bespalova, N. B.; Finkeishtein, E. Sh.; Bondar, V. I.; Popov, A. V. *Macromolecules* **1994**, *27*, 2872.
(29) Widom, B. *J. Chem. Phys.* **1963**, *39*, 2802.
(30) Frenkel, D.; Smit, B. *Understanding Molecular Simulation*; Academic Press: San Diego, CA, 1996.

MA0480751